TERMINAL-AREA THROUGHPUT: MEASURING CAPACITY AND ROBUSTNESS

Terence R. Thompson and Michael Brennan , Metron Aviation, Herndon, VA, USA

S. Bradford and D. Liang, FAA/ASD-100, Washington, D.C., USA

Abstract

Measurement of terminal-area capacity has been addressed via historical analysis of the observed throughput in different segments of the terminal area encompassing four New York airports (EWR, JFK, LGA, and TEB). Localized throughput has been measured in terms of maximum observed values for segments of the terminal area and in terms of sub-maximal values observed when neighboring segments are operating at maximum total throughput.

System robustness was investigated by simulating weather-related closures of segments of the terminal area. Traffic was transferred from closed segments to neighboring segments, and the frequency with which these transfers exceeded maximal and sub-maximal capacity thresholds was calculated. Analysis of these frequencies provides a measure of robustness with respect to weather-related reductions in capacity, and provides a quantitative basis for plans to handle such reductions in capacity.

The overall objective of this work is to benchmark the capacity of different terminals and to compare benchmarks for airports and terminals.

Introduction

Terminal-area capacity and robustness in the face of airspace closures is one of several pressing issues in improving the efficiency of the U.S. National Airspace System (NAS). Airport capacity is relatively well understood [1], but terminal and en route capacities are not. Prediction of emerging problems in NAS behavior, as well as generation of control strategies that are robust in the face of uncertainty both require better understanding of the capacity of spatially distinct, but linked elements of the NAS. We are engaged in efforts to characterize this capacity in both the terminal and en route domains, and we report on the terminal area work here.

Methods and Results

The principal elements in the terminal-area work reported here were data assembly, capacity estimation, and quantification of robustness via emulation of traffic transfers.

Data Assembly

A circular boundary approximately 50 nautical miles in radius centered on EWR was used to define the terminal airspace, and radar tracks for February, April, and July of 2000 were assembled. Figure 1 shows this traffic, color-coded by airport, with the 8 boundary segments.

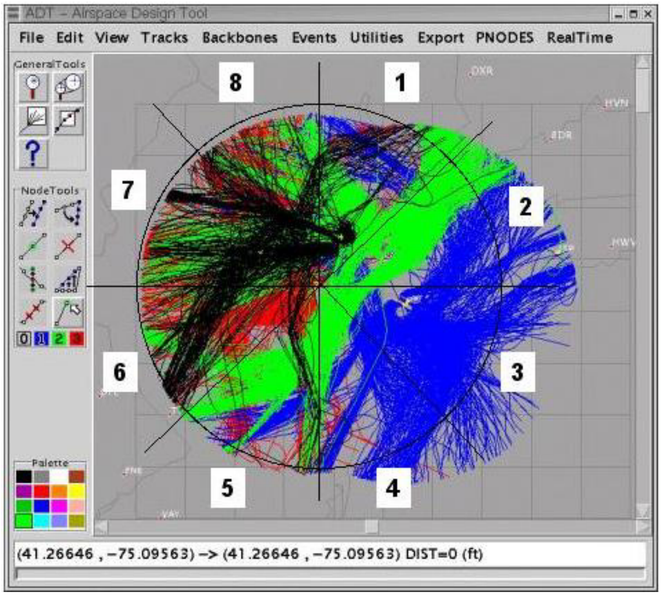

```
(41.26646 , -75.09563) -> (41.26646 , -75.09563) DIST=0 (ft)
```

Figure 1. Traffic for 1 February 2000 with Overlay of Eight Boundary Segments (red=EWR, green=LGA, blue=JFK, black=TEB)

Eight 45-degree segments on this boundary were defined (extending from the ground to 50,000 feet MSL), and the entry or exit segment for each of the 295,000 flights in the data set was determined. Traffic inbound to or outbound from EWR, JFK, LGA, and TEB was included, but other traffic was not represented in the data set.

In effect, a ring has been drawn around the terminal area, and the spatial distribution of flux of traffic (for the four major airports) into and out of the terminal area has been measured. This ring could be drawn at different distances from the center of the terminal area, but 50 nautical miles was chosen as a convenient distance for purposes of this study. Table 1 shows the traffic counts for each segment of the ring.

Table 1. Percentage of Total Traffic in Each Segment and Arrival/Departure Percentage

Segment	Percent of Total	Arr. Percent	Dep. Percent
1	11.1	38.1	61.9
2	8.8	60.1	39.9
3	3.4	4.7	95.3
4	6.2	80.6	19.4
5	15.2	44.5	55.5
6	19.8	59.1	40.9
7	21.7	40.4	59.6
8	13.8	45.8	54.2

Capacity Estimation

Throughput was defined as the total number of arriving and departing aircraft crossing each segment boundary. This throughput was calculated for each 15-minute time period over each of the 90 days of data, and statistics of throughput for each segment were analyzed. The total number of observations of throughput was 8640 (24 hours/day x 4 periods/hour x 90 days).

Total throughput for all eight segments was distributed as shown in Figure 2. The maximum total throughput was 106, and the 95th-percentile value was 64.

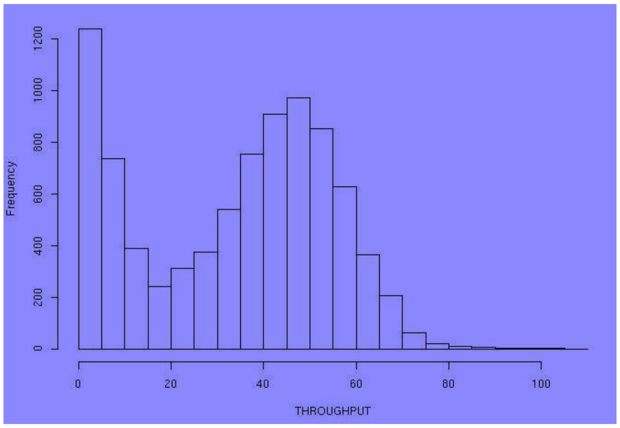

Figure 2. Histogram of Total Terminal-area Throughput for Each 15-minute Time Period (n=8640; max=106)

XXX Explain how we are looking for "max" capacity, not average capacity. Use hist6.jpg.

Maximum values of throughput for each segment were determined. In addition, a subset (n=446) of the 8640 operations was defined in which the total throughput was greater than or equal to 64, the 95th-percentile value of the total throughput (XXX explain that this is the same when low values are dropped). For this "high total throughput" subset, the 95th-percentile value of each segment's throughput was calculated. These values are shown in the second and third columns of Table 2.

Table 2. Individual Segment Throughput Values (95th-percentile values for high total throughput)

Segment	Max.	95th-Per. (15 min)	95th-Per. (30 min.)
1	15	12	11
2	17	12	11
3	11	6	5.5
4	12	8	7.5
5	18	14	13
6	25	20	19
7	27	20	19.5

8	21	16	15
Total	146	108	101.5

In order to test whether the throughput values for individual segments were sensitive to the size of the time bin used, the 95th-percentile value was also calculated for 30-minute time bins, rather than 15-minute bins. The resulting values, given in the third column of Table 2, show that the 30-minute values were only slightly lower than the 15-minute values. This indicates that the capacities measured for 15-minute bins are not abnormally high values that cannot be maintained for at least two time periods. For this reason all further analysis used only 15-minute time bins.

XXX Simple intro; maybe mention servers being dependent in network of queues. Use runway analogy. XXX Since neighboring segments may be inter-dependent in terms of their capacity, simultaneous throughput for each set of three neighboring segments was analyzed to quantify this linkage. Each triplet's maximum total throughput was found (n=446), and the values of the individual segment throughputs at this maximal triplet throughput were determined. Table 3 shows the results of this analysis

Table 3. Segment Throughput Values Observed at Maximum Triplet Throughput

Triplet Segment	123	234	345	456	567	678	781	812
1	15	-	-	-	-	-	15	15
2	15	15	-	-	-	-	-	15
3	5	5	6	-	-	-	-	-
4	-	11	8	8 11	-	-	-	-
5	-	-	16	16 11	15	-	-	-
6	-	-	-	20 22	23	23 20	-	-
7	-	-	-	-	21	20 16	18	-
8	-	-	-	-	-	14 21	14	14
Triplet Maximum	35	31	30	44	59	57	47	44

In two cases (triplets 456 and 678), there were multiple observations that gave the same maximum triplet throughput. For the 678 triplet, Figures 3, 4, and 5 plot individual segment throughputs versus the total throughput for the triplet.

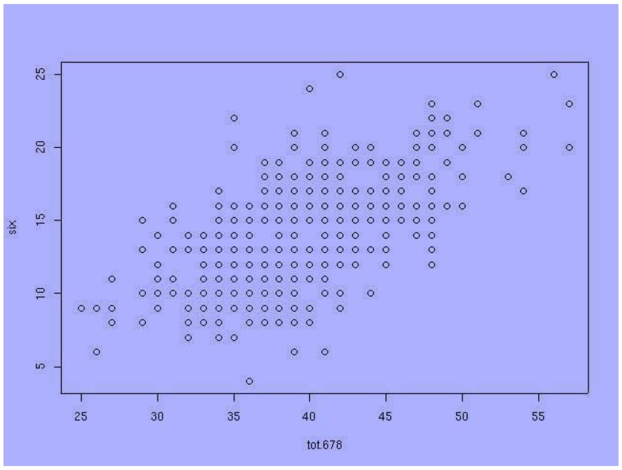

Figure 3. Throughput of Segment 6 Versus Total Throughput for Segments 6, 7, and 8. (maximal triplet throughput=57; segment 6 values 20, 23)

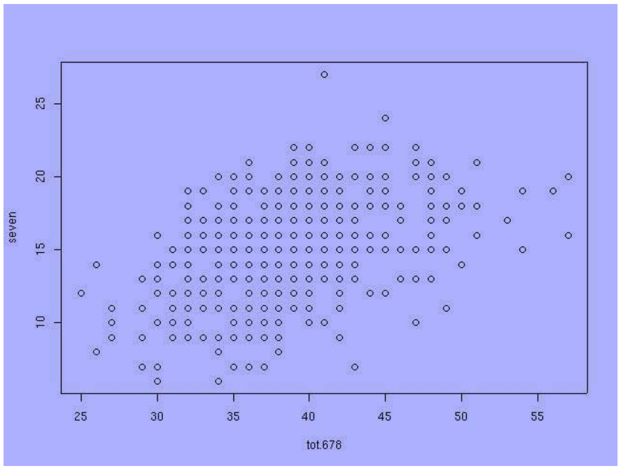

Figure 4. Throughput of Segment 7 Versus Total Throughput for Segments 6, 7, and 8. (maximal triplet throughput=57; segment 6 values 16, 21)

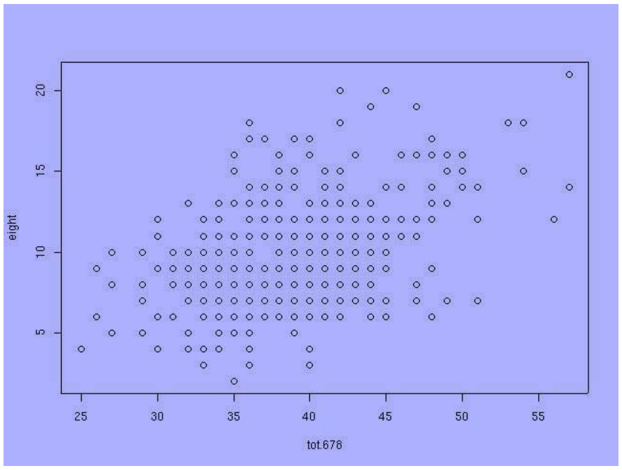

Figure 6. Throughput of Segment 8 Versus Total Throughput for Segments 6, 7, and 8. (maximal triplet throughput=57; segment 6 values 14, 21)

XXX Motivational intro sentence. XXX This data can now be used to identify XXX conservative ???XXX useful sub-maximal operating points for each segment. Comparing the values in Table 3 to the second and third columns of Table 2, we see that: XXX make easier to follow from Table 3 XXX

(1) When the total throughput is high (greater than 95th-percentile value of 64) and a given triplet is operating at its maximum, segments 1-6 operate at or above their own observed 95th-percentile (high-total) value. However, segments 7-8 operate somewhat below this value.

(2) In the same circumstances, segment 1 operates at its maximum observed value, while segments 2-8 operate well below the maximum value.

XXX Make this explanation of how to get sub-max values clearer. XXX A set of sub-maximal operating points consistent with this data (XXX and the two constraining observations above) is given in the last column of Table 4. These were calculated by averaging (and rounded) the values for each sector from Table 3.

Table 4. Comparison of Sub-maximal Operating Points with Maximum and 95th-percentile Values

Segment	**Maximum**	**95th Per.**	**Sub-maximal**
1	15	12	15
2	17	12	15
3	11	6	5
4	12	8	8
5	18	14	15
6	25	20	21
7	27	20	19
8	21	16	15
Total	146	108	113

The results in Table 4 show that there are significant variations in the terminal-area segment capacities that may be related to the current structure and organization of airspace elements.

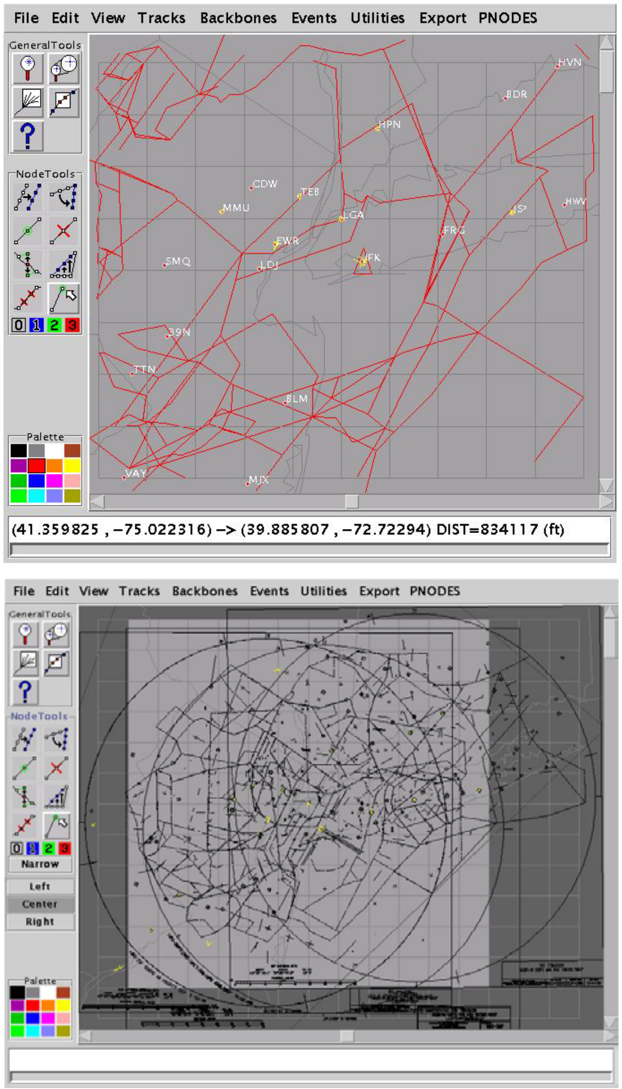

(41.359825 , −75.022316) −> (39.885807 , −72.72294) DIST=834117 (ft)

Figure 7. ZNY Sectors and Video Overlays XXX Need to update

The results in Table 4 also indicate that an overall terminal area capacity could be estimated using 20 aircraft per 15-minute period for each of the 8 segments, or 160 aircraft per 15-minute period for the entire terminal area.

Robustness Estimation via Traffic Transfers

Weather-related closures of segments of the terminal area were simulated by transferring traffic from the closed segment to neighboring segments. Using the maximal and sub-maximal segment-specific throughput values as thresholds, the frequency with which these transfers exceeded the throughput thresholds was calculated as a measure of the robustness of the terminal-area capacity. Robustness is here considered to be the ability to absorb the transfers without exceeding the thresholds. XXX Make sure that new reader understands this. Use no-smoking graphic.

Traffic transfers were simulated under different conditions by setting three different parameters to various values:

(1) Use of maximal or sub-maximal segment capacities;
(2) Transfer of traffic to one neighboring segment or to two neighboring segments. and
(3) Transfer of different percentages of traffic between segments.

In all, XXX simulations were conducted.

For example, using maximal throughput capacities, transfer of traffic from segment 7 to segment 8 at three transfer percentages gave the results shown in Figures 8 (100% transfer), 9 (70% transfer), and 10 (50% transfer). The transfers were made, individually, for each of the 15-minute periods in the 90-day database described above, so there were 8640 simulated transfer instances. These figures plot the frequency with which the traffic transfer “failed”, that is, the frequency with which capacity was exceeded in the segment receiving the transferred traffic.

Each month of data was treated separately in these simulations to maintain visibility of monthly variability in the results. The blue line in each graph shows the average over all three months of data

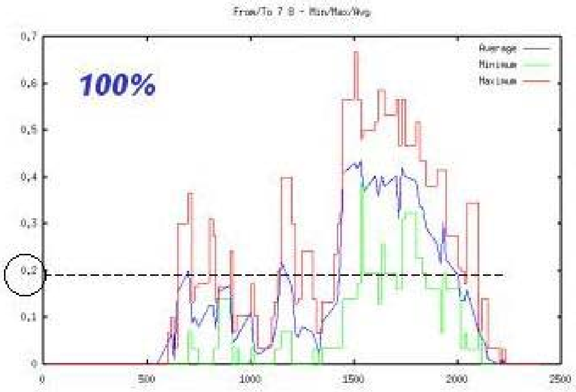

Figure 8. Frequency of Transfer of 100% of Traffic From Segment 7 Exceeding Maximal Threshold for Segment 8 (frequency vs. GMT; n=8640; blue=average across 3 single months)

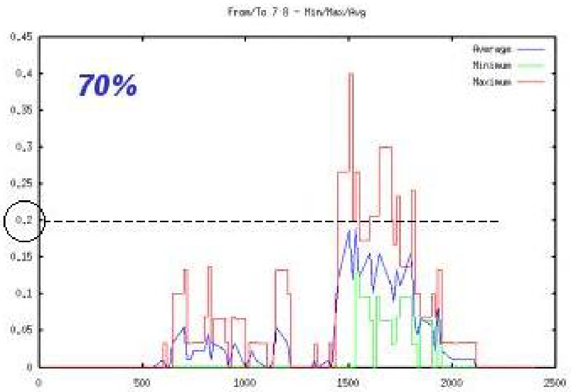

Figure 9. Frequency of Transfer of 70% of Traffic From Segment 7 Exceeding Maximal Threshold for Segment 8 (frequency vs. GMT; n=8640; blue=average across 3 single months)

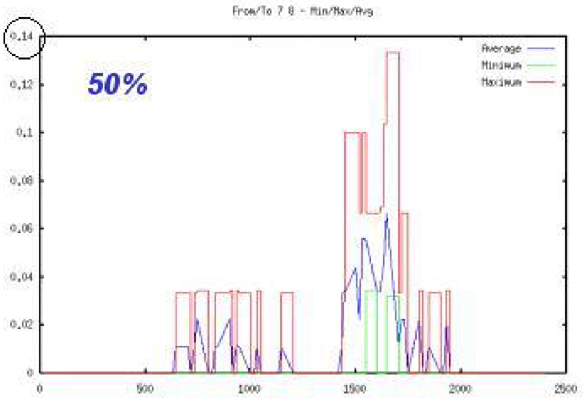

Figure 10. Frequency of Transfer of 50% of Traffic From Segment 7 Exceeding Maximal Threshold for Segment 8 (frequency vs. GMT; n=8640; blue=average across 3 single months)

The principal simulations are summarized in Tables 5a and 5b. These tables shows the source segment, the receiving segment, the percentage of traffic transferred, the capacity assumed for the receiving segment, the 24-hour failure frequency, and the 5-hour failure frequency for the "peak-traffic" 1500-2000 period. For each source segment, 6 simulations are summarized, as follows:

- 100% transfer to the *left* neighbor using either maximal or sub-maximal capacity for the receiving segment (2 simulations);
- 100% transfer to the *right* neighbor using either maximal or sub-maximal capacity for the receiving segment (2 simulations); and
- 50% transfer to *both the left and right* neighbors using either maximal or sub-maximal capacity for the receiving segment (2 simulations);

Table 5a. Summary of Traffic-transfer Simulations for Source Segments 1-4 (values above 0.2 in red)

Src	Rcvr	Pct	Cap	FR24	FR5 (peak)
1	8	100	Max	0.009	0.033
			Sub	0.116	0.306
	2	100	Max	0.014	0.040
			Sub	0.039	0.114
	2/8	50/50	Max	0.002	0.006
			Sub	0.029	0.087
2	1	100	Max	0.039	0.114
			Sub	0.039	0.114
	3	100	Max	0.021	0.074
			Sub	0.338	0.660
	3/1	50/50	Max	0.006	0.022
			Sub	0.109	0.302
3	2	100	Max	0.001	0.004
			Sub	0.003	0.011
	4	100	Max	0.003	0.009
			Sub	0.038	0.112
	4/2	50/50	Max	0.001	0.003
			Sub	0.012	0.035

4	3	100	Max	0.005	0.015
			Sub	0.203	0.468
	5	100	Max	0.008	0.023
			Sub	0.044	0.106
	5/3	50/50	Max	0.001	0.006
			Sub	0.076	0.202

Table 5b. Summary of Traffic-transfer Simulations for Source Segments 5-8 (values above 0.2 in red)

Src	Rcvr	Pct	Cap	FR24	FR5 (peak)
5	4	100	Max	0.167	0.330
			Sub	0.445	0.759
	6	100	Max	0.028	0.071
			Sub	0.115	0.249
	6/4	50/50	Max	0.011	0.033
			Sub	0.147	0.342
6	5	100	Max	0.243	0.467
			Sub	0.396	0.689
	7	100	Max	0.068	0.218
			Sub	0.318	0.649
	7/5	50/50	Max	0.031	0.075
			Sub	0.230	0.566
7	6	100	Max	0.111	0.324
			Sub	0.238	0.546
	8	100	Max	0.120	0.354
			Sub	0.364	0.730
	8/6	50/50	Max	0.017	0.059
			Sub	0.150	0.454
8	7	100	Max	0.019	0.069
			Sub	0.188	0.499
	1	100	Max	0.116	0.306
			Sub	0.116	0.306
	1/7	50/50	Max	0.012	0.040
			Sub	0.073	0.237

Analysis of the frequencies in Tables 5a and 5b provides a measure of the robustness of the system to weather-related reductions in capacity and provides a quantitative basis for plans to handle such reductions in capacity. For example:

- Using maximal throughput values, failure rates for 50/50 transfers are below 0.2 for all segments. In other words, significant robustness (using maximum throughput values) throughout the day.
- Using sub-maximal throughput values, failure rates for 50/50 transfers are above 0.23 only in the 1500-2000 period. In other words, little robustness (using sub-maximal throughput values) during peak-traffic periods.
- XXX More XXX

Overall, we conclude that there is little robustness in terminal-area capacity during peak periods using the sub-maximal estimate of segment capacity.

Conclusions and Next Steps

This work has shown that it is feasible to use large numbers of observations of throughput to derive terminal area capacity, both for localized segments and for the overall terminal area. It has also developed and applied a means of estimating the robustness of the localized terminal-area capacity to traffic transfers that might be necessary to avoid weather problems or other restrictions on local throughput.

Next steps in this work include the following:

- Analysis of similar traffic transfers using separate arrival and departure flows.
- More detailed analysis of the relation of the segments to current airspace elements; and
- Extension to en route airspace elements.

XXXFigure 7 shows the approximate relationship of the segments analyzed and the current sector (XXX videomap ???) structure.
XXX Need to say something intelligent here about the relation of the 8 segments to the airspace structures. MOVE THIS TO FUTURE WORK.

References

[1] Gilbo, E. P., 1993, “Airport Capacity: Representation, Estimation, Optimization”, IEEE Transactions on Control Systems Technology, 1(3):144-54.

[2] Donahue, G. L., and Laska, W. D., 2001, “United States and European Airport Capacity Assessment Using the GMU Macroscopic Capacity Model”, in *Air Transportation Systems Engineering (Progress in Astronautics and Aeronautics, Volume 193)*, Donahue, G., and Zellweger, A., editors, AIAA, Reston, Virginia, pp. 61-73.

[3] Voss, W. M., and O’Rourke, A. L., 2002, “Redefining the Scope of Terminal Airspace”, in *Proceedings ATM 2002 Advanced Workshop*, Capri, Italy, Galati and Zellweger, editors, pp. 133-141.

[4] Bradford, S., Knorr, D., and Liang, D., 2001, “Performance Measures for Future Architecture”, in *Air Transportation Systems Engineering (Progress in Astronautics and Aeronautics, Volume 193)*, Donahue, G., and Zellweger, A., editors, AIAA, Reston, Virginia, pp.397-407.

[5] Voss, W., and Joffman, J., 2001, “Analytical Identification of Airport and Airspace Capacity Constraints”, in *Air Transportation Systems Engineering (Progress in Astronautics and Aeronautics, Volume 193)*, Donahue, G., and Zellweger, A., editors, AIAA, Reston, Virginia, pp.409-421.

Keywords

Terminal area

Capacity estimation

Robustness

Simulation of capacity loss

Biographies

<u>Dr. Terence R. Thompson</u> is Vice President for Research and Development Technology at Metron Aviation. He leads the NAS Genome Project and his research focuses on the behavior of the NAS as a complex system, airspace design, route optimization, and aircraft-noise modeling. His Ph.D. work was completed at the University of Rochester in the area of computational biophysics.

<u>Michael Brennan</u> is the Chief Scientist for Metron Aviation, Inc (MAI), in Herndon, Virginia, and Technical Manager of the Technology and Infrastructure Division there. He received a B.S. in Physics from the University of Pennsylvania and an M.S. in Computer Science and Operations Research from Villanova University. He is responsible for the conceptual development and validation of mid- to near-term TFM innovations at MAI. As chief scientist, he also oversees the coordination and technical quality of all of MAI’s analysis and research efforts. Mr. Brennan has been involved in aviation for six years, and prior to that worked on analysis and decision aids for the Department of Defense.

<u>Steve Bradford</u> is the Chief Scientist for Architecture and NAS Development in the FAA's Office of System Architecture and Investment Analysis (ASD). In this role he has participated in the development of the RTCA NAS Operational Concept and the ICAO ATMCP Global Concept. His organization is also responsible for leading the effort to validate the future concepts, develop the FAA's ATC Information Architecture and leads several co-operative efforts via action plans with Eurocontrol. Prior to his current position, Mr. Bradford was the Manager of the NAS Concept

Development Branch. Earlier, Mr. Bradford was lead on several simulation and analytic software development efforts, and conducted early analysis of Free Flight Concepts.

Diana Liang works for the Office of System Architecture and Investment Analysis for the Architecture and System Engineering Division. She is responsible for the development of the NAS Architecture Tool and Interface called CATS-I, directing analyses in support of NAS Concept Validation, and the development of Modeling Tools and Fast-Time Simulations to support that validation. This work includes several models she is developing jointly with NASA and cooperative efforts with Europe via Eurocontrol. Prior to working for ASD, Ms. Liang worked in the Office of Energy and Environment for two years as the lead for the Emissions and Dispersion Modeling System (EDMS).